

IDENTIFICATION OF ACTIVE MAGNETIC BEARING SYSTEM USING MAGNETIC FORCE MEASUREMENT

Chong-Won Lee

Center for Noise and Vibration Control(NOVIC), Department of Mechanical Engineering
Korea Advanced Institute of Science and Technology, Science Town, Taejon, Korea

Young-Ho Ha

Daewoo Precision Industries Ltd., Pusan, Korea

Cheol-Soon Kim

Samsung Advanced Institute of Technology, Suwon, Korea

ABSTRACT

An active magnetic bearing(AMB) system is developed, which is equipped with two sets of piezoelectric-type force transducers so that in-plane forces generated by a pair of magnetic bearings can be measured. Each magnetic bearings are mounted on each set of force transducers, consisting of four shear-type cells.

In the process of modal testing, the radial bearings in the stabilized closed loop system are excited by the random and sinusoidal voltage inputs to power amplifiers, and then the forces and displacements at the bearings are measured simultaneously, all quantities being defined in the complex domain. The modal properties of AMB system are then effectively identified from directional frequency response functions (dFRFs) defined between the complex inputs and outputs. It is shown that we can also identify the position and current stiffnesses from the relations between forces, displacements and currents.

INTRODUCTION

Active magnetic bearings (AMBs) have been increasingly interesting for industrial applications because of the advantages of non-contact, elimination of lubrication, low power loss and controllability of the bearing dynamic characteristics[1-2]. Typical industrial application fields include turbomachinery, space or vacuum technology, bearings in machine tools, etc. After an AMB system is constructed, an important issue for designers is to investigate whether the system behaves in accordance with the original design analysis of the closed loop system[3]. AMB systems often show discrepancies between the predicted and the measured dynamic behaviors due to the inaccurate modeling

associated with the magnetic forces, frequency characteristics of the power amplifiers and control coils, leakage and fringing effects of the magnetic fluxes, eddy current effects, etc. Thus accurate system parameter identification is essential in order to improve the system performance and stability.

In this paper, two sets of piezoelectric-type force transducers measure in-plane forces generated by a pair of magnetic bearings. The measured force signals can be used as a useful and essential information for accurate system parameter identification. The modal properties of the AMB system are effectively identified from directional frequency response functions(dFRFs) obtained by the complex modal testing. It has been well known that, whereas both forward and backward modes in the classical FRFs appear over one-sided frequency region, resulting in overlapping of the otherwise physically well separated modes, they are completely separated in the dFRFs[4-8].

DIRECTIONAL FREQUENCY RESPONSE FUNCTIONS FOR AMB SYSTEM

The use of complex coordinate has been proven very convenient in rotor dynamic analysis because it allows rather straightforward physical interpretation and it reduces the order of equations of motion by one half for axisymmetric rotor systems [4-8]. The complex modal analysis, which has been developed for rotating machinery, based on the use of complex coordinates, clearly defines the backward and forward modes and separates them in the frequency domain so that the effective modal parameter identification is possible.

Equation of Motion in Complex Domain

Consider a rigid rotor magnetic bearing system, which can be modeled as a symmetric rigid rotor

supported by two anisotropic bearings as shown in FIGURE 1.

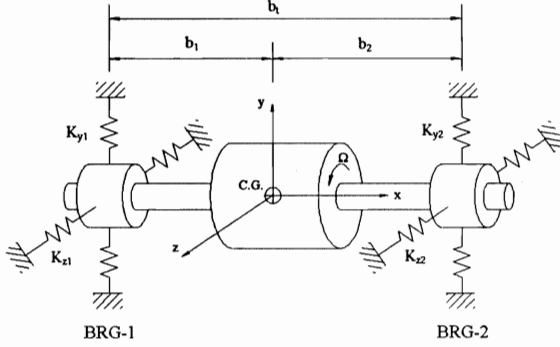


FIGURE 1: Rigid rotor active magnetic bearing system

The equation of motion in complex domain can be written at each bearing locations as

$$\begin{aligned} \mathbf{M}_f \ddot{\mathbf{p}}(t) + [\mathbf{C}_g + \mathbf{C}_f] \dot{\mathbf{p}}(t) + \mathbf{C}_b(t) \bar{\mathbf{p}}(t) \\ + \mathbf{K}_f \mathbf{p}(t) + \mathbf{K}_b \bar{\mathbf{p}}(t) = \mathbf{g}(t), \end{aligned} \quad (1)$$

where j means the imaginary number ($=\sqrt{-1}$) and the bar denotes the complex conjugate. Here the complex-valued system matrices, displacement and force vectors are defined as

$$\begin{aligned} \mathbf{p}(t) &= \begin{Bmatrix} p_1(t) \\ p_2(t) \end{Bmatrix} = \begin{Bmatrix} y_1(t) + jz_1(t) \\ y_2(t) + jz_2(t) \end{Bmatrix}, \\ \mathbf{g}(t) &= \begin{Bmatrix} g_1(t) \\ g_2(t) \end{Bmatrix} = \begin{Bmatrix} f_{y_1}(t) + jf_{z_1}(t) \\ f_{y_2}(t) + jf_{z_2}(t) \end{Bmatrix}, \\ \mathbf{M}_f &= \begin{bmatrix} m\ell_2^2 + i_d & m\ell_1\ell_2 - i_d \\ m\ell_1\ell_2 - i_d & m\ell_1^2 + i_d \end{bmatrix}, \\ \mathbf{C}_g &= \begin{bmatrix} -j\Omega i_p & j\Omega i_p \\ j\Omega i_p & -j\Omega i_p \end{bmatrix}, \end{aligned}$$

$$i_d = I_d/b_i^2, \quad i_p = I_p/b_i^2, \quad \ell_i = b_i/b_t, \quad i=1,2,$$

$$\begin{aligned} \mathbf{C}_f &= \begin{bmatrix} c_1 & 0 \\ 0 & c_2 \end{bmatrix}, \quad \mathbf{C}_b = \begin{bmatrix} \Delta c_1 & 0 \\ 0 & \Delta c_2 \end{bmatrix} \\ \mathbf{K}_f &= \begin{bmatrix} k_1 & 0 \\ 0 & k_2 \end{bmatrix}, \quad \mathbf{K}_b = \begin{bmatrix} \Delta k_1 & 0 \\ 0 & \Delta k_2 \end{bmatrix} \end{aligned} \quad (2)$$

$$\begin{aligned} 2c_i &= c_{yy_i} + c_{zz_i} - j(c_{yz_i} - c_{zy_i}), \\ 2\Delta c_i &= c_{yy_i} - c_{zz_i} - j(c_{yz_i} + c_{zy_i}), \\ 2k_i &= k_{yy_i} + k_{zz_i} - j(k_{yz_i} - k_{zy_i}), \\ 2\Delta k_i &= k_{yy_i} - k_{zz_i} + j(k_{yz_i} + k_{zy_i}), \end{aligned}$$

In the above expressions, m is the total mass of the rotor, I_p and I_t are the diametrical and polar mass moment of inertia about the center of gravity (C.G.) of the rotor, respectively, b_t is the bearing span, $b_i, i=1,2$, is the distance of the i -th bearing from C.G., and c_{ij} and $k_{ij}, i,j=y,z$, are the damping and stiffness coefficients of the two anisotropic bearings.

Directional frequency response functions

Taking Fourier transform of equation (1), we obtain

$$\begin{bmatrix} \mathbf{D}_f & \mathbf{D}_b \\ \hat{\mathbf{D}}_b & \hat{\mathbf{D}}_f \end{bmatrix} \begin{Bmatrix} \mathbf{P}(j\omega) \\ \hat{\mathbf{P}}(j\omega) \end{Bmatrix} = \begin{Bmatrix} \mathbf{G}(j\omega) \\ \hat{\mathbf{G}}(j\omega) \end{Bmatrix}, \quad (3)$$

where $\mathbf{P}(j\omega), \hat{\mathbf{P}}(j\omega), \mathbf{G}(j\omega)$ and $\hat{\mathbf{G}}(j\omega)$ are the Fourier transforms of $\mathbf{p}(t), \bar{\mathbf{p}}(t), \mathbf{g}(t)$ and $\bar{\mathbf{g}}(t)$, respectively, and the partitioned dynamic stiffness matrices are

$$\mathbf{D}_f(j\omega) = \mathbf{K}_f - \omega^2 \mathbf{M}_f + j\omega(\mathbf{C}_f + \mathbf{C}_g),$$

$$\mathbf{D}_b(j\omega) = \mathbf{K}_b + j\omega \mathbf{C}_b$$

$$\hat{\mathbf{D}}_b(j\omega) = \bar{\mathbf{K}}_b + j\omega \bar{\mathbf{C}}_b,$$

$$\hat{\mathbf{D}}_f(j\omega) = \bar{\mathbf{K}}_f - \omega^2 \bar{\mathbf{M}}_f + j\omega(\bar{\mathbf{C}}_g + \bar{\mathbf{C}}_f).$$

From equation (3), the two-sided directional frequency response matrices (dFRMs) are defined as

$$\begin{Bmatrix} \mathbf{P}(j\omega) \\ \hat{\mathbf{P}}(j\omega) \end{Bmatrix} = \begin{bmatrix} \mathbf{H}_{gp}(j\omega) & \mathbf{H}_{\hat{g}p}(j\omega) \\ \mathbf{H}_{g\hat{p}}(j\omega) & \mathbf{H}_{\hat{g}\hat{p}}(j\omega) \end{bmatrix} \begin{Bmatrix} \mathbf{G}(j\omega) \\ \hat{\mathbf{G}}(j\omega) \end{Bmatrix}, \quad (4)$$

where

$$\mathbf{H}_{gp}(j\omega) = [\mathbf{D}_f - \mathbf{D}_b \hat{\mathbf{D}}_f^{-1} \hat{\mathbf{D}}_b]^{-1},$$

$$\mathbf{H}_{\hat{g}p}(j\omega) = [\hat{\mathbf{D}}_f - \hat{\mathbf{D}}_d \mathbf{D}_f^{-1} \mathbf{D}_b]^{-1},$$

$$\mathbf{H}_{g\hat{p}}(j\omega) = -[\mathbf{D}_f - \mathbf{D}_b \hat{\mathbf{D}}_f^{-1} \hat{\mathbf{D}}_b]^{-1} \mathbf{D}_b \hat{\mathbf{D}}_f^{-1},$$

$$\mathbf{H}_{\hat{g}\hat{p}}(j\omega) = -[\hat{\mathbf{D}}_f - \hat{\mathbf{D}}_d \mathbf{D}_f^{-1} \mathbf{D}_b]^{-1} \hat{\mathbf{D}}_d \mathbf{D}_f^{-1}.$$

Here $\mathbf{H}_{gp}(j\omega)$ and $\mathbf{H}_{\hat{g}p}(j\omega)$ are referred to as the normal dFRMs whereas $\mathbf{H}_{g\hat{p}}(j\omega)$ and $\mathbf{H}_{\hat{g}\hat{p}}(j\omega)$ are referred to as the reverse dFRMs [4,7]. From equations (3) and (4), it can be easily proven that

$$\mathbf{H}_{g\hat{p}}(j\omega) = \bar{\mathbf{H}}_{\hat{g}p}(-j\omega), \quad \mathbf{H}_{\hat{g}\hat{p}}(j\omega) = \bar{\mathbf{H}}_{gp}(-j\omega). \quad (5)$$

Therefore, in order to define the dFRMs completely, it is sufficient to consider two dFRMs, i.e.

$$\mathbf{P}(j\omega) = \begin{bmatrix} \mathbf{H}_{gp}(j\omega) & \mathbf{H}_{\hat{g}p}(j\omega) \end{bmatrix} \begin{Bmatrix} \mathbf{G}(j\omega) \\ \hat{\mathbf{G}}(j\omega) \end{Bmatrix}. \quad (6)$$

It has been well known that, for an isotropic AMB system, the reverse dFRMs vanish, i.e.

$$\mathbf{H}_{g\hat{p}}(j\omega) = \mathbf{H}_{\hat{g}\hat{p}}(j\omega) = \mathbf{0}. \quad (7)$$

FIGURE 2 shows the simple two-complex input/single-complex output model. From FIGURE 2,

when $g(t)$ and $\bar{g}(t)$ are not fully coherent, dFRFs associated with complex inputs and output of the AMB system can be estimated from [4-7]

$$H_{gp}(j\omega) = \frac{S_{gp}(j\omega)}{S_{gg}(j\omega)} \frac{1 - \frac{S_{\hat{g}p}(j\omega)S_{\hat{g}\hat{g}}(j\omega)}{S_{\hat{g}p}(j\omega)S_{\hat{g}\hat{g}}(j\omega)}}{1 - \gamma_{\hat{g}\hat{g}}^2(j\omega)},$$

$$H_{\hat{g}p}(j\omega) = \frac{S_{\hat{g}p}(j\omega)}{S_{\hat{g}\hat{g}}(j\omega)} \frac{1 - \frac{S_{gp}(j\omega)S_{\hat{g}\hat{g}}(j\omega)}{S_{\hat{g}p}(j\omega)S_{\hat{g}\hat{g}}(j\omega)}}{1 - \gamma_{\hat{g}\hat{g}}^2(j\omega)}, \quad (8)$$

where $S_{ik}(j\omega)$, $i, k = p, g, \hat{g}$, are the two-sided directional auto- and cross-spectral density functions (dPSDs and dCSDs) between the complex time signals, $p(t)$, $g(t)$ and $\bar{g}(t)$, respectively, and $\gamma_{\hat{g}\hat{g}}^2(j\omega)$ is the directional coherence function (dCOH) between the complex inputs, $g(t)$ and $\bar{g}(t)$, defined as

$$\gamma_{\hat{g}\hat{g}}^2(j\omega) = \frac{|S_{\hat{g}\hat{g}}(j\omega)|^2}{S_{gg}(j\omega)S_{\hat{g}\hat{g}}(j\omega)}. \quad (9)$$

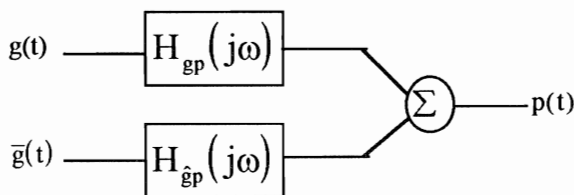


Fig. 2 Two-complex input/single-complex output model

EXPERIMENTAL SET UP AND PROCEDURE

FIGURE 3 shows an AMB system equipped with two sets of piezoelectric-type force transducers so that in-plane forces generated by a pair of magnetic bearings can be measured. Each set of force transducers consists of four shear type cells, on which radial magnetic bearings are mounted. The AMB system is stabilized by P-D digital controller with a DSP board. Linearizing the magnetic force w.r.t. the neutral position, the net magnetic force $f(t)$ due to small perturbations, $p(t)$, in air gap and, $i_c(t)$, in control current, can be expressed as

$$f(t) = K_i i_c(t) + K_q p(t), \quad (10)$$

where K_i, K_q are the current and position stiffnesses, respectively. Since it is difficult to directly control the current, the conversion of voltage to current is achieved through the power amplifiers [6,8]. Approximating the

magnetic actuator including the PWM amplifier and electromagnets as a first order delay element, we can express the control current to voltage relationship in Laplace domain as

$$i_c(s) = \frac{K_c}{1 + \tau_c s} v_c(s) \quad (11)$$

where v_c, τ_c and K_c are the control voltage, the time constant and the gain of the magnetic actuator, respectively.

FIGURE 4 shows the block diagram for parameter identification of the AMB system, where two independent band limited random noise (0-400Hz) or sinusoidal excitation signals (25 Hz) are applied to the input ports of the power amplifiers for simultaneous excitations in the y- and z- directions of the stabilized closed loop system. The displacements are perturbed due to the excitation forces generated in electromagnets. Two pairs of gap sensors measure the y- and z- directional displacements of the shaft at bearings # 1 and # 2, giving two-complex responses (or two pairs of real responses), and the excitation forces are measured by the two sets of force transducers. The force, displacement and excitation voltage records are processed in the LMS signal analyzer, and stored for further processing.

RESULTS AND DISCUSSION

A series of preliminary tests are performed in order to accurately identify the physical parameters of the AMB system. Among others, the current and position stiffnesses, which are the important parameters affecting the control performance of the AMB system, should first be accurately estimated [8]. Analyzing sinusoidal signals in time and frequency domains, we can calculate the current and position stiffnesses from equations (10) and (11). In equation (11), the input voltage is estimated from the excitation and sinusoidal control voltages of digital controller. TABLE 1 gives the rotor specifications, and compares the computed and identified actuator properties. The discrepancy between the measured and computed values is found to be larger for K_q than for K_i , the measured values being smaller than the computed ones. It implies that the actual equivalent air gap is larger than the design value. With the magnet parameters determined, the modal properties of the rotor bearing system are identified through a series of complex modal testing in order to accurately model the closed loop system. FIGURES 5 and 6 are the real and imaginary plots of the normal and reverse dFRFs at bearing #1, respectively, at the rotational speed of 6800 rpm (114 cps). The figures indicate that the residues in the reverse dFRF are about one eighth in magnitude of the

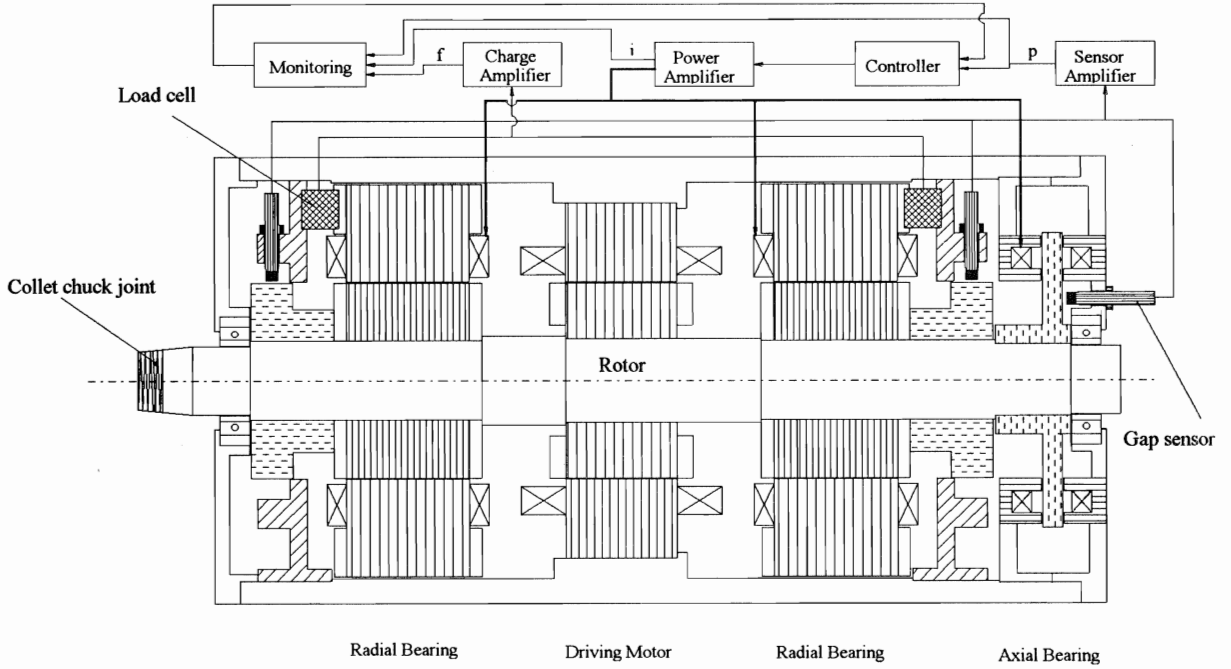


FIGURE 3: AMB system equipped with force transducers

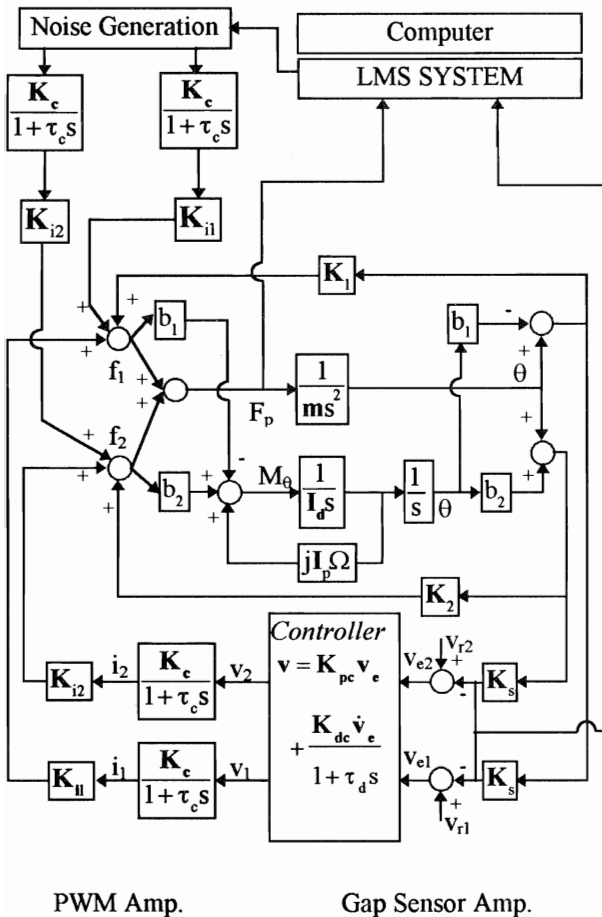


FIGURE 4: Block diagram for parameter identification of AMB system

normal dFRF, implying that the tested AMB system is weakly anisotropic in nature. Unlike the classical FRFs, FIGURE 5 shows the complete separation of the forward and backward modes, i.e. the forward modes on the positive frequency region

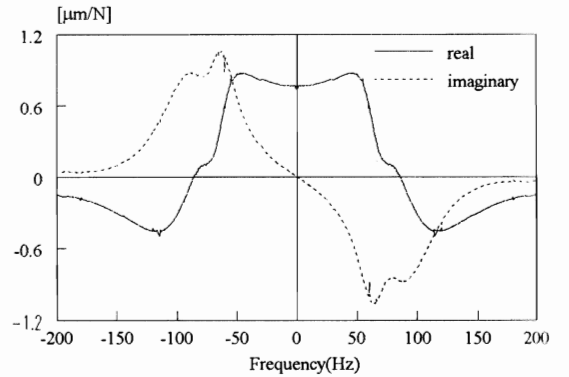


FIGURE 5: Real/Imaginary Plots of normal dFRFs(H_{g1p1}) at Bearing #1, $\Omega = 6800$ rpm

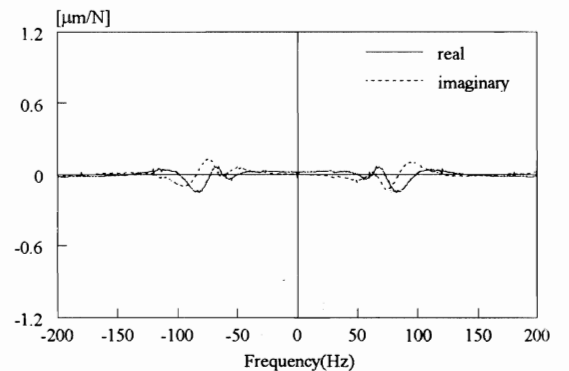


FIGURE 6: Real/Imaginary Plots of reverse dFRFs(H_{g1p1}) at Bearing #1, $\Omega = 6800$ rpm

and the backward modes on the negative frequency region. Therefore the accuracy of the modal parameter extraction is much improved. TABLE 2 summarizes the modal parameters extracted from multi-mode curve fit of measured dFRFs, along with the computational results for comparison. Note that the calculated and identified modal frequencies are in good agreement. But the identified damping ratios are found to be smaller than the computed ones. The discrepancy may take place due to the unmodeled system parameters such as time delays associated with low-pass filters, nonlinearity of magnetic force, eddy current effect, leakage, etc.

TABLE 1: Specification of Rotor and Properties of Actuators

Rotor		
m : 9.66 kg	I_d : 0.1089 kg-m ²	
I_p : 0.00725 kg-m ²	b_1 : 0.172 m	
b_1 : 0.101 m	b_2 : 0.071 m	

Actuator		
properties	identified	computed
Current Stiffness (N/A)		
K_{iy1}	288	305
K_{iz1}	286	305
K_{iy2}	283	300
K_{iz2}	280	300
Position Stiffness (N/m)		
K_{qy1}	1.21E6	1.38E6
K_{qz1}	1.19E6	1.38E6
K_{qy2}	1.14E6	1.33E6
K_{qz2}	1.13E6	1.33E6

TABLE 2: Identified and Computed Modal Parameters (F=forward mode, B=back mode)

Mode	Identified		Computed	
	ω_n (Hz)	ζ	ω_n (Hz)	ζ
1F	70.1	0.25	73.3	0.41
1B	66.8	0.17	67.3	0.40
2F	94.0	93.1	93.1	0.49
2B	91.7	0.17	92.0	0.49

CONCLUSION

An AMB system is developed, which is equipped with two sets of piezoelectric force transducers, can measure in-plane forces generated by a pair of magnetic bearings. Using measured sinusoidal force, displacement and voltage signals, we can easily identify the current and position stiffnesses. Using the dFRFs defined between the excitation and displacement signals, the system modal properties can also be effectively identified. The comparison between the computed and identified properties suggests that unmodeled system properties or inaccurate modelling may lead to poor estimation of system parameters such as position and current stiffnesses and system modal dampings.

REFERENCES

1. H. Habermann and G. Liard, An active magnetic bearing system, *TRIBOLOGY international* April 1980, p85-89
2. H. Ulbrich, New Test Techniques Using Magnetic Bearings, Proc. of the 1st Int. Symp. on Magnetic Bearings, ETH Zurich, Switzerland, 1988
3. R. R. Humphris, A Device for Generating Diagnostic Information for Rotating Machinery Using Magnetic Bearings, Proc. of MAG'92, Magnetic Bearings, Magnetic Drives and Dry Gas Seals Conference & Exhibition, Virginia, 1992
4. C.W. Lee, Vibration Analysis of Rotors, Kluwer Academic publishers, 1993
5. C.W. Lee, A Complex Modal Testing Theory for Rotating Machinery, *Mech. Sys. and Signal Processing*, Vol. 5, No. 2, p119-1137, 1991
6. Y.D. Joh and C.W. Lee, Excitation Methods and Modal parameter Identification in Complex Modal Testing for Rotating Machinery, "Int'l J. Analysis & Experimental Modal Analysis. Vol. 8, No. 3 p178-203, 1993
7. C.W. Lee and C.Y. Joh, Theoretical Development in the Use of the dFRF for Diagnosis of Anisotropy and Asymmetry in Rotating Machinery, *Mech. Sys. and Signal Processing*, Vol. 8, No. 6, 1994 (to appear)
8. C.W. Lee and J.S. Kim, Modal Testing and Suboptimal Vibration control of Flexible Rotor Bearing System by Using a Magnetic Bearing, *J. Dynamic Systems Measurement and Control*, Vol. 114, p244-252, June, 1992

